DOI 10.1007/s10517-016-3466-3
Cell Technologies in Biology and Medicine, No. 2, August, 2016

Internalization of Vectored Liposomes in a Culture of Poorly Differentiated Tumor Cells

P. A. Mel'nikov[1], V. P. Baklaushev[1], A. N. Gabashvili[1], N. V. Nukolova[1,2], A. B.Levinsky[2], and V. P. Chehonin[1,2]

Translated from *Kletochnye Tekhnologii v Biologii i Meditsine*, No. 2, pp. 115-121, April, 2016
Original article submitted April 21, 2015

Internalization of liposomal nanocontainers conjugated with monoclonal antibodies to VEGF, VEGFR2 (KDR), and proteins overproduced in the tumor tissue was studied *in vitro* on cultures of poorly differentiated tumor cells. Comparative analysis of accumulation of vectored liposomes in the tumor cells was performed by evaluating co-localization of labeled containers and cell organelles by laser scanning confocal microscopy. We observed nearly 2 times more active penetration and accumulation of liposomes vectored with antibodies in the tumor cells in comparison with non-vectored liposomes. Selective clathrin-dependent penetration of vectored liposomes into tumor cells was demonstrated by using pharmacological agents inhibiting endocytosis.

Key Words: *internalization; liposomes; targeted delivery; monoclonal antibodies to VEGF and VEGFR2 (KDR); glioma*

Liposomal systems are effective nanocontainers for delivery of chemotherapeutic drugs and negatively charged agents (microRNA, viral and non-viral agents) to tumor cells [3,8,13]. Pegylated liposomes covalently bound to monoclonal antibodies to surface antigens of tumor cells provide selective delivery of drugs directly to the tumor focus [6]. Well-known peculiarities of the vascular bed of brain tumors (hypervascularization, enhanced vascular permeability, and violation of the blood—brain barrier integrity) promote penetration and accumulation of nanocontainer preparation with a diameter of 150-200 nm in the tumor tissue [1,7,11].

The final molecular target of nanocontainer forms of intercalating antitumor drugs and therapeutic genes is nuclear DNA of the corresponding target cells. Therefore, internalization of the nanocontainer, release of active substance into the cytoplasm and/or intracellular organelles, and its penetration into the cell nucleus are the key mechanisms that determine the effectiveness of the targeted delivery of the nanobiotechnological preparation [12]. The mechanism of endocytosis predetermines the fate of absorbed nanocontainer (whether the content will appear in late endosomes or will be released into the cytoplasm), and the solution to the problem of internalization of targeted nanocontainers can significantly diversify the approaches to effective intracellular delivery. Transmembrane transport and further release of the preparation are influenced by a number of factors, including chemical structure, size, charge, and shape of the nanocontainer as well as properties of vector molecule [2,4,5].

The choice of the target specific for tumor cells and accessible for vector molecule is the key problem in targeted delivery of the nanocontainer preparation. In our study, monoclonal antibodies to surface markers of tumor cell VEGF receptor type 2 (VEGFR2, KDR) and to VEGF were used as vectors for targeted delivery. Overexpression of genes encoding VEGF and its receptor in tumor cells was shown for many malignant tumors, including glioblastoma multiforme [10].

Conjugation of the nanocontainer with the monoclonal antibody to surface marker should theoretically

[1]Department of Medical Nanobiotechnologies, Medico-Biological Faculty, N. I. Pirogov National Research Medical University; [2]Department of Fundamental and Applied Neurobiology, V. P. Serbsky Federal Medical Research Centre for Psychiatry and Narcology, Ministry of Health of the Russian Federation, Moscow, Russia. ***Address for correspondence:*** proximopm@gmail.com. P. A. Mel'nikov

provide stable fixation of the nanocontainer on the target cell surface due to antigen–antibody interaction. However, further transport of the nanocontainer bound to this or that membrane protein into the cell remains poorly studied.

We studied the mechanisms of internalization of fluorescence-labeled non-vectored and vectored immune liposomes conjugated with monoclonal antibodies to KDR and VEGF into C6 glioma and adenocarcinoma cells.

MATERIALS AND METHODS

Synthesis of liposomal systems. The first stage in the synthesis of nanocontainers was preparation of multilamellar liposomes from lecithin, cholesterol, DSPE-PEG, and DDAB. These components were dissolved in chloroform:methanol (2:1) mixture in a molar ratio of 20, 10, 1.5 and 0.35-10 (the content of cationic lipid depended on the required surface charge of the final product). In a round bottom flask, 1.5 ml lecithin (10 mg/ml, 20 μmol) was mixed with 3.9 mg cholesterol. DSPE-PEG (50 mg/ml) was added for the formation of additional "spikes" on the liposome surface to reduce their opsonization and to prolong circulation longevity of the developed liposome systems in the blood. For preparation of 1% cationized liposomes, 15 μl DDAB in chloroform (10 mg/ml) was added. For synthesis of more charged systems (5, 10, and 25%), 75, 150, and 375 μl DDAB was added. For fluorescent labeling, lipophilic dye Dil/DiD in chloroform (10 mg/ml) or FITC was added to liposomal emulsion according to manufacturer's protocol. The mixture was placed on a rotary evaporator controlled by an automatic vacuum pump. For complete elimination of the residual solvent (especially methanol that prevents liposome formation during subsequent hydration), evaporation was carried out at flasks rotation speed of 270 rpm, 40 μbar pressure, and water bath temperature 40°C for 1 h, which led to the formation of a thin lipid film on the round-bottom flask wall and its lyophilization. Then, 2 ml warm distilled water (30°C) was added to the flask and vortexed until complete homogenization; the resulting suspension was then left at room temperature for 1 h for the formation of multilamellar liposomes. To obtain unilamellar liposomes, the suspension was subjected to emulsification by repeated freezing/thawing cycles in liquid nitrogen (~10 times) followed by 10-min sonication. The resultant clear liposome solution was left at room temperature for 1-2 h.

Synthesis of vectored liposomal systems. Monoclonal antibodies were thiolated prior to binding with liposomes. To this end, antibody solution (1-5 mg in 1 ml 0.1 M carbonate buffer (pH 8.0) containing 2 mM EDTA) was incubated with 10-fold molar excess of 2-iminothiolate (Traut's reagent) for 1 h. After incubation, free Traut's reagent and by-products were separated from the activated antibody by gel chromatography on a NAP-10 column with Sephadex G-25 pre-equilibrated with PBS containing 2 mM EDTA. Thiolated protein was immediately used for conjugation with liposomes. Liposomes containing maleimide groups should be immediately used for conjugation, because maleimide groups in solution undergo hydrolysis (hydrolysis rate increases with increasing pH).

For conjugation, activated antibodies were mixed with freshly prepared liposomes at a ratio of 45 nM antibodies per 20 μM lecithin (PBS, pH 7.5). The mixture was incubated for 4 h at room temperature or overnight at 4°C. The reaction was stopped by adding 100-fold molar excess (relative to protein) of 2-mercaptoethanol that blocks free sulfhydryl groups. Immune liposomes were separated from other reaction components and unbound monoclonal antibodies by gel filtration on Sepharose CL-4B (~1×50 cm) equilibrated with 20 mM PBS (pH 7.4) containing 150 mM NaCl. The obtained liposomes were concentrated by centrifugation at 1000*g* using CentriFlo CF50 membrane cones.

Characterization of liposomes. The hydrodynamic diameter, polydispersity index, and surface charge (ζ-potential) of liposomes were determined by dynamic light scattering on a Zetasizer Nano ZS ZEN 3500 instrument (Malvern Instruments Ltd) in a Size&Zeta potential folded capillary cell (DTS1060). For measurements, the liposomes were dissolved in distilled water to a lipid concentration 5 mg/ml. Mean values for all samples were calculated from at least 3 measurements, the data are presented as mean±standard deviation. Liposome stability was evaluated by measuring the hydrodynamic radius and polydispersity index over time by dynamic light scattering.

Immunochemical activity of anti-VEGF-liposomes was determined by ELISA. The concentration of antibodies bound with liposomes was determined by measuring total protein concentration using a Coomassie Protein Assay kit.

Preparation of cell cultures. C6 cells were cultured in DMEM/F-12 medium (Gibco) supplemented with 5% fetal calf serum and antibiotics in 25-cm^2 plastic flasks (Corning) at 37°C in humidified atmosphere with 5% CO_2. During passaging, the cells were harvested with 0.25% trypsin–EDTA (Gibco). Cell organelles were visualized using LysoTracker Red DND-99, CellLight Lysosomes GFP, and BacMam 2.0 (Molecular Probes).

Experimental design. C6 cells were passaged in 35-mm Petri dishes (5×10^3 cells per dish). After attaining 50% confluence, lysosomes were stained according to instructions of LysoTracker Red DND-99 (560 nm)

or Lysosomes-GFP, BacMam 2.0 (488 nm) manufacturers. Then, the cells were washed with serum-free medium, liposomes (50 μg/ml phosphatidylcholine), 5 μg/ml antibodies to VEGF, KDR, and Avastin were added. Non-vectored liposomes and liposomes conjugated with IgG served as the control. The final concentration of the added preparation was calculated based on the intensity of liposome fluorescence measured on an EnSpire microplate analyzer. The cells were incubated with the added preparations in humidified atmosphere at 37°C and 5% CO_2 for 15, 30, and 60 min, washed three times in Dulbecco's modification PBS (Gibco), and placed in a chamber for intravital microscopy.

Analysis of the mechanisms of internalization of liposomal systems in a culture of C6 cells using endocytosis inhibitors. Clathrin-mediated endocytosis was inhibited with chlorpromazine acting on AP-2 complex and thereby preventing the assembly of clathrin lattice of the primary endosome. Chlorpromazine was incubated with the cells before addition of the nanocontainer in concentrations of 10, 5, 2.5, and 1.25 μM for 2-4 h. Then, the cells were gently washed and incubated with liposomes for 1 h [2].

Caveolin-dependent endocytosis was blocked with methyl-β-cyclodextrin. This inhibitor prevents assembly of caveolae by affecting caveolin-1 through the formation of cholesterol complexes. In our experiments, C6 cells were incubated in 5, 2.5, 1.25 μM inhibitor solutions for 2 h, gently washed, and incubated with liposomes for 1 h.

Confocal microscopy. Scanning was performed using a Nikon A1R MP+ confocal laser scanning microscope. Lasers with emission at 405, 488, 561, and 638 nm and objectives Plan Apo 20x/0.75 Dic N, Apo IR 60x/1.27 WI, and Apo TIRF 60x/1.49 oil Dic were used. The cell contours were visualized by differential interference contrast.

RESULTS

At the first stage of the study, we prepared fluorescence-labeled cationized liposomal nanocontainers with PEG-modified surface preventing their uptake by macrophages, which significantly increases their nanocontainer circulation [9] in the blood. Then, we prepared vectored nanocontainers containing monoclonal antibodies to VEGF, KDR, and Avastin (humanized antibody to VEGF; Roche) acting as vectors. Mouse IgG was used as a non-specific vector (Table 1).

Dynamic light scattering analysis of physicochemical parameters of immune liposome nanocontainers showed that liposome preparations conjugated with specific and unspecific antibodies have similar mean diameter (from 170 to 186 nm), charge (from -2.1 to -3.7 mV), and polydispersity index (0.06-0.09). Non-vectored liposomes did not differ from vectored liposomes by polydispersity index and charge, but had smaller mean diameter (146.00±0.13 nm) due to the absence of antibodies on their surface (Table 1).

In the analysis of internalization of vectored liposomes labeled with DiD (ex 647 nm) or FITC (ex 488 nm), we performed dynamic scanning of cells after 10-60-min incubation (with 10-min intervals) and then after 90-min incubation for the analysis of the dynamics of liposome trafficking across the membrane. The experiment was performed on low-differentiated glioma C6 cells with lysosomes labeled with LysoTracker Red DND-99. Intracellular localization of immunoliposomes was confirmed by co-localization analysis of fluorescent signals from nanocontainers and from labeled organelles. During image processing using NIS-Elements AR software, we calculated cell number, their area, and fluorescence intensity. This analysis allowed excluding fluorescent signals of the particles not entering the cytoplasm and restrained on the plasmolemma surface.

TABLE 1. Physicochemical Characteristics of Experimental Liposome Preparations (*M*±*m*)

Vector	Liposome diameter, nm	ζ-potential, mV	Polydispersity index (PDI)	Fluorescent label
Anti-VEGF	186.00±0.22	-2.3	0.09±0.03	DiD (ex 647 nm), FITC (ex 488 nm)
Anti-KDR	176.00±0.17	-2.1	0.06±0.03	DiD (ex 647 nm), FITC (ex 488 nm)
Avastin	180.00±0.21	-2.4	0.06±0.02	DiD (ex 647 nm), FITC (ex 488 nm)
IgG	170.00±0.23	-3.7	0.07±0.03	DiD (ex 647 nm), FITC (ex 488 nm)
Without vector molecule	146.00±0.13	-3.8	0.10±0.03	DiD (ex 647 nm), FITC (ex 488 nm)

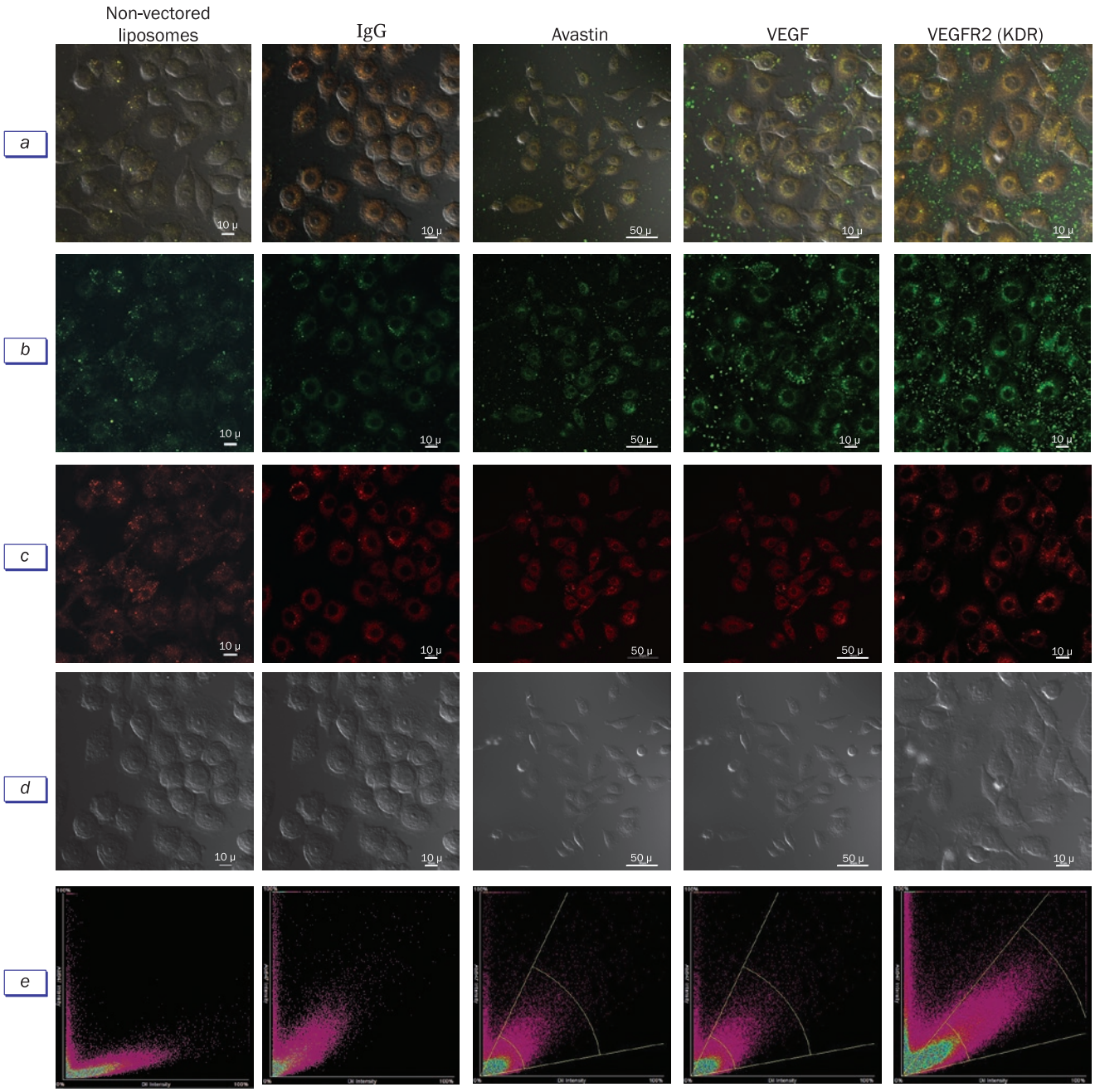

Fig. 1. Internalization of vectored liposomes in C6 glioma cells. *a*) Superposition of images; *b*) liposomal dye FITC; *c*) LysoTracker Red DND-99; *d*) differential interference contrast microscopy; *e*) co-localization analysis (scatter plot); abscissa: intensity of LysoTracker Red DND-99 fluorescence in lysosomes (red channel), ordinate: FITC fluorescence (green channel).

The performed dynamic analysis of internalization of labeled immune liposomes within 60 min after their addition to glioma cells showed that the rate of internalization of vectored and non-vectored liposomes considerably differed. Immune liposomes with vector antibodies to VEGF, KDR, and Avastin were detected in cells as soon as after 30-min incubation. In case of non-vectored liposomes with IgG, the intracellular signals appeared in 40 min, whereas intracellular localization of liposomes containing no antibodies was detected after 60-min incubation (Fig. 1).

Co-localization analysis of immune liposomes with labeled lysosomes after 60-min incubation confirmed that culture of C6 cells most actively internalized nanocontainers vectored with antibodies to VEGF and KDR. The results of co-localization analysis are presented as Pearson's linear correlation plots (Fig. 1, *e*). The linear correlation coefficients for immune liposomes with anti-VEGF, anti-KDR, Avastin, IgG,

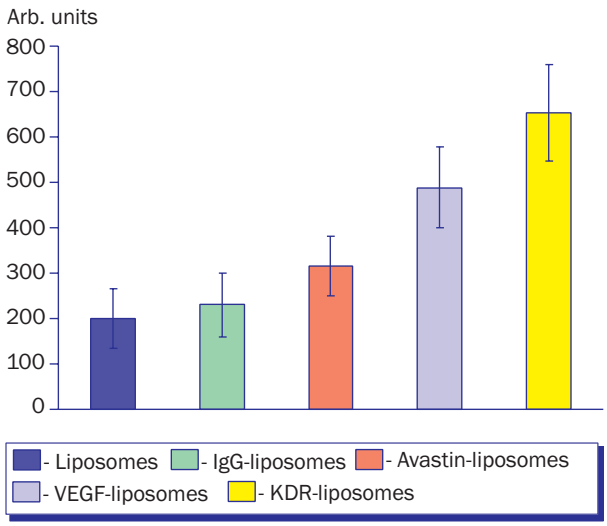

Fig. 2. Mean intensity of intracellular fluorescence of vectored and non-vectored immune liposomes.

and non-vectored liposomes were 0.58, 0.46, 0.6, 0.46, and 0.43, respectively. In these co-localization plots, the intensity of intracellular fluorescence of vectored and non-vectored immune liposomes differed significantly (Fig. 1, *e*).

After NIS-Elements AR processing of more than 500 cells in the experiments for each type of nanocontainer, the mean intensity of intracellular fluorescence for vectored and non-vectored nanocontainers was obtained. The intracellular fluorescence intensity was maximum after incubation of C6 glioma cells with VEGF and KDR-immune liposomes (488.3 and 651.1 arb units, respectively). Liposomes conjugated with Avastin showed almost half as high intracellular fluorescence as KDR-conjugated liposomes. The intensity of intracellular fluorescence of immune liposomes with unspecific IgG and non-vectored liposomes was 233.4 and 206.7 arb. units, respectively, *i.e.* 2-fold lower than that of VEGF-conjugated immune liposomes and almost 3-fold lower than the corresponding parameter for KDR-conjugated immune liposomes (Fig. 2).

The results of analysis of internalization rate and intensity of intracellular fluorescence of immune liposome nanocontainers in *in vitro* experiments on cultured poorly differentiated glioma C6 cells characterized by high chemoresistance suggest that vector immune liposome system based on monoclonal antibodies to VEGF and KDR more effectively (by 2 and 3 times in comparison with non-vectored liposomes, respectively) penetrate into the cell and can provide higher bioavailability of the nanocontainer form of intercalating agent or genetic material.

The next task was elucidation of the mechanisms of immune liposome internalization with the use of various endocytosis inhibitors. Visualization of lysosomes in this case was carried out using the BacMam technology: C6 culture cells were incubated for 1 day with modified baculovirus; C6 glioma cell transfection led to *GFP* gene expression in lysosomes. The cells were incubated with 5 and 10 mM chlorpromazine, inhibitor of clathrin-mediated endocytosis, for 2-4 h before addition of the nanocontainer. Then, the cells were gently washed and incubated with liposomes for 1 h. This experiment showed that blockade of clathrin-mediated endocytosis almost completely abolished internalization of nanocontainers vectored with specific monoclonal antibodies to VEGF and KDR into cultured C6 glioma cells (Fig. 3). Pearson's correlation coefficient in co-localization analysis in this case was 0.1 for VEGF- and KDR-conjugated immune liposomes. These results attest to selective clathrin-mediated endocytosis of vectored immune liposomes based on monoclonal antibodies to VEGF and KDR.

It is noteworthy that in a similar experiment with non-vectored liposomes and liposomes conjugated

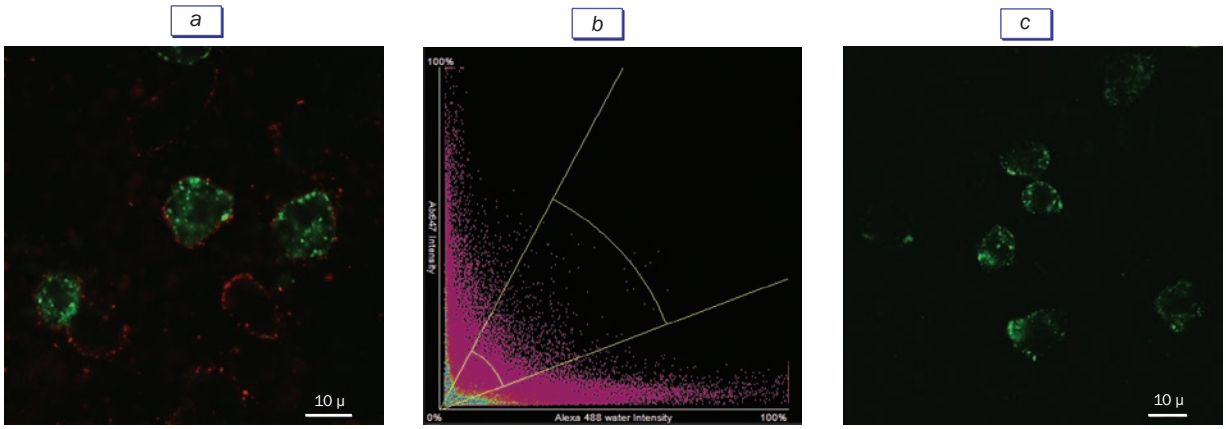

Fig. 3. Blockade of internalization of immunoliposomes vectored by monoclonal antibodies to VEGF and VEGFR2 with inhibitor of clathrin-mediated endocytosis chlorpromazine. *a*) VEGF-immune liposomes; *b*) co-localization histogram, *c*) KDR-immune liposomes. Complete absence of co-localization of nanocontainers (red channel; abscissa) and lysosomes (green channel; ordinate).

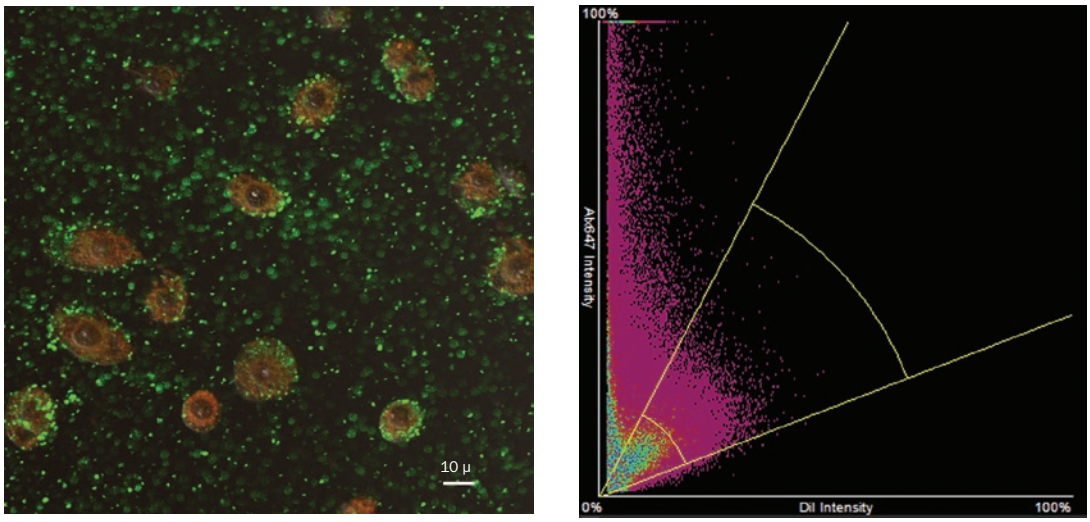

Fig. 4. Internalization of non-vectored liposomes and immune liposomes with unspecific IgG in the presence of an inhibitor of clathrin-mediated endocytosis chlorpromazine. Partial internalization of liposomes with unspecific vector and non-vectored liposomes. Nanocontainers (green channel; abscissa) and lysosomes (red channel; ordinate).

with IgG, their internalization into the cells in the presence chlorpromazine changed insignificantly. Co-localization analysis in this case showed partial localization of non-vectored nanocontainers on the cells membrane and in lysosomes. Thus, we can assume different mechanisms of endocytosis of vectored and non-vectored immune liposomes (Fig. 4).

In similar experiments with methyl-β-cyclodextrin (inhibitor of caveolin-mediated endocytosis), internalization of both vectored and non-vectored liposomes was observed in the presence of this inhibitor. This drove us to a conclusion that caveolin-mediated endocytosis plays minor role in intracellular delivery of immune liposomes.

The study showed that vectored immune liposome nanocontainers carrying monoclonal antibodies to VEGF, KDR, and Avastin significantly more effectively penetrated into poorly differentiated chemoresistant C6 glioma cells than non-vectored nanocontainers. Targeted nanocontainers are more rapidly internalized and the intensity of intracellular fluorescence in this case increased by more than 2 times (in case of liposomes with anti-KDR-antibodies by almost 3 times) in comparison with non-vectored liposomes. Vector liposomes are internalized into C6 glioma cells by the mechanism of clathrin-mediated endocytosis. On the contrary, caveolin-mediated mechanism plays minor role in liposome internalization. Liposomes with nonspecific vector and non-vectored liposomes apparently penetrate into C6 cells via both clathrin-mediated endocytosis and other unspecific mechanisms. Our results can be used for creation of new more sophisticated preparations for intracellular delivery of antitumor drugs and genetic material.

The author are grateful to S. A. Shein and A. A. Korchagina for provided monoclonal antibodies to VEGF and KDR.

The study was supported by the Russian Science Foundation (grant No. 14-04-00882; synthesis of nanocontainers; grant No. 14-15-00698; work with cell cultures and confocal microscopy).

REFERENCES

1. Baklaushev VP, Nukolova NN, Khalansky AS, Gurina OI, Yusubalieva GM, Grinenko NP, Gubskiy IL, Melnikov PA, Kardashova KSh, Kabanov AV, Chekhonin VP. Treatment of glioma by cisplatin-loaded nanogels conjugated with monoclonal antibodies against Cx43 and BSAT1. Drug Deliv. 2015;22(3):276-285.
2. Bannunah AM, Vllasaliu D, Lord J, Stolnik S. Mechanisms of nanoparticle internalization and transport across an intestinal epithelial cell model: effect of sizeand surface charge. Mol. Pharm. 2014;11;(12):4363-4373.
3. Estanqueiro M, Amaral MH, Conceição J, Sousa Lobo JM. Nanotechnological carriers for cancer chemotherapy: the state of the art. Colloids Surf. B Biointerfaces. 2015;126:631-648.
4. Gratton SE, Ropp PA, Pohlhaus PD, Luft JC, Madden VJ, Napier ME, DeSimone JM. The effect of particle design on cellular internalization pathways. Proc. Natl Acad. Sci. USA. 2008;105(33):11,613-11,618.
5. Kibria G, Hatakeyama H, Ohga N, Hida K, Harashima H. The effect of liposomal size on the targeted delivery of doxorubicin to Integrin αvβ3-expressing tumor endothelial cells. Biomaterials. 2013;34(22):5617-5627.
6. Korchagina AA, Shein SA, Leopol'd AV, Volgina NE, Gurina OI, Lazarenko IP, Antonova OM, Baklaushev VP, Chekhonin VP. Generation of recombinant extracellular fragment of vascular endothelial growth factor receptor 2 and specific mono-

clonal antibodies to this receptor. Bull. Exp. Biol. Med. 2014;156(3):357-362.
7. Maeda H, Wu J, Sawa T, Matsumura Y, Hori K. Tumor vascular permeability and the EPR effect in macromolecular therapeutics: a review. J. Control. Release. 2000;65(1-2):271-284.
8. Minko T, Pakunlu RI, Wang Y, Khandare JJ, Saad M. New generation of liposomal drugs for cancer. Anticancer Agents Med. Chem. 2006;6(6):537-552.
9. Neupane M, Clark AP, Landini S, Birkbak NJ, Eklund AC, Lim E, Culhane AC, Barry WT, Schumacher SE, Beroukhim R, Szallasi Z, Vidal M, Hill DE, Silver DP. MECP2 Is a Frequently Amplified Oncogene with a Novel Epigenetic Mechanism That Mimics the Role of Activated RAS in Malignancy. Cancer Discov. 2016;6(1):45-58. doi: 10.1158/2159-8290.CD-15-0341.
10. Reardon DA, Wen PY, Desjardins A, Batchelor TT, Vredenburgh JJ. Glioblastoma multiforme: an emerging paradigm of anti-VEGF therapy. Expert Opin. Biol. Ther. 2008;8(4):541-453.
11. Shein SA, Nukolova NV, Korchagina AA, Abakumova TO, Kiuznetsov II, Abakumov MA, Baklaushev VP, Gurina OI, Chekhonin VP. Site-directed delivery of VEGF-targeted liposomes into intracranial C6 glioma. Bull. Exp. Biol. Med. 2015;158(3):371-376.
12. Yameen B, Choi WI, Vilos C, Swami A, Shi J, Farokhzad OC. Insight into nanoparticle cellular uptake and intracellular targeting. J. Control. Release. 2014;190:485-499.
13. Zhang J, Li X, Huang L. Non-viral nanocarriers for siRNA delivery in breast cancer. J. Control. Release. 2014;190:440-450.